

NACA TN 3326

**CASE FILE
COPY**

**NATIONAL ADVISORY COMMITTEE
FOR AERONAUTICS**

TECHNICAL NOTE 3326

**THE COMPRESSIBLE LAMINAR BOUNDARY LAYER WITH HEAT
TRANSFER AND ARBITRARY PRESSURE GRADIENT**

By Clarence B. Cohen and Eli Reshotko

**Lewis Flight Propulsion Laboratory
Cleveland, Ohio**



Washington
April 1955

THE COMPRESSIBLE LAMINAR BOUNDARY LAYER WITH HEAT

TRANSFER AND ARBITRARY PRESSURE GRADIENT

By Clarence B. Cohen and Eli Reshotko

SUMMARY

An approximate method for the calculation of the compressible laminar boundary layer with heat transfer and arbitrary pressure gradient, based on Thwaites' correlation concept, is presented. The method results from the application of Stewartson's transformation to Prandtl's equations, which yields a nonlinear set of two first-order differential equations. These equations are then expressed in terms of dimensionless parameters related to the wall shear, the surface heat transfer, and the transformed free-stream velocity. Thwaites' concept of the unique interdependence of these parameters is assumed. The evaluation of these quantities is then carried out by utilizing exact solutions recently obtained.

With the resulting relations, methods are derived for the calculation of the two-dimensional and axially symmetric laminar boundary layer with an arbitrary free-stream velocity distribution, Mach number, and surface temperature.

The combined effect of heat transfer and pressure gradient is demonstrated by applying the method to calculate the characteristics of the boundary layer on thin supersonic surfaces and in a highly cooled, convergent-divergent, axially symmetric rocket nozzle.

INTRODUCTION¹

In recent years, with the advent of laminar airfoils and with the observation of laminar boundary layers at Reynolds numbers as high as 50×10^6 (ref. 2), the ability to reliably estimate viscous flow and heat-transfer effects for a laminar boundary layer has become increasingly

¹The principal developments of this paper, which is part of the doctoral dissertation of the senior author (ref. 1), were carried out under the stimulus and guidance of Professor Luigi Crocco and the sponsorship of the Daniel and Florence Guggenheim Foundation. The final analysis and the computations were completed at the NACA Lewis laboratory.

important. Moreover, with high-altitude flight becoming more common, the subsequent lower Reynolds numbers encountered should more frequently produce a laminar boundary layer. Stability calculations based on the theory of Lees and Lin (ref. 3) have also emphasized the possibilities of maintaining a laminar boundary layer through cooling of aerodynamic surfaces. The effect of favorable pressure gradients in increasing the stability of laminar boundary layers may also make solutions to the laminar problem applicable to the design of nozzles and turbine blades.

Solution of the laminar-boundary-layer equations which include effects of compressibility, pressure gradient, and heat transfer have been quite limited in number. Of the exact solutions, most have restrictions of range or application, or both. The solutions of references 4 and 5 are restricted to zero pressure gradient, while those of reference 6 allow small pressure gradients. The developments of reference 7 are restricted to small heat transfer and low Mach number. Solutions obtained by assuming that fluid properties are constant or that the Mach number is essentially zero are obtained in references 8 to 10. Those solutions of references 11 and 12 that are for a Prandtl number of unity are not restricted in range of compressibility, pressure gradient, or heat transfer. However, they apply to specific types of free-stream velocity distribution which are inappropriate for general practical problems.

In 1921, von Kármán (ref. 13) recognized that to solve the skin-friction problem it was not necessary to have the exact and complicated solution, but that it would be quite satisfactory to evaluate average quantities across the layer if they could be related to the surface values. The concepts of displacement and momentum thicknesses were introduced, thus considerably simplifying the mathematics of the problem. With this integral method, if the form of the velocity profile is related to a single parameter, a method of calculating the boundary layer is obtained. Pohlhausen (ref. 14) carried out this method by postulating a quartic velocity profile depending upon the local pressure gradient. A number of investigators have extended Pohlhausen's method to compressible flows over insulated surfaces.

With the presence of heat transfer at the surface, the compressible problem becomes more complex. Kalikhman (ref. 15) defined certain heat-flow quantities analogous to the displacement and momentum thicknesses and, in a manner similar to Pohlhausen's, developed a complex iterative procedure for the solution of the general problem. More recently, references 16 to 19 have further developed this technique. The preceding methods are tedious, since they require a solution of at least one ordinary differential equation for any particular problem.

Thwaites' method (ref. 20) does not require the solution of ordinary differential equations. In that formulation, it is suggested that

the basic goal of an integral approach might be achieved if the problem is considered as that of relating the wall shear, its normal derivative at the wall, and the form factor (ratio of displacement thickness) to one another without specifying a type of profile. To this end, nondimensional forms of these quantities were defined and were evaluated by examining exact solutions for the incompressible laminar boundary layer. It developed that a nearly universal relation existed between these quantities for favorable pressure gradients and, for adverse pressure gradients, Thwaites selected a single representative relation. A unique correlation was chosen which reduced the solution of an incompressible problem to the evaluation of a single integral.²

Rott and Crabtree (ref. 22) recognized that, in the absence of heat transfer and with a Prandtl number of unity, the Illingworth-Stewartson correlation between compressible and incompressible boundary-layer solutions (ref. 23) could be used to extend Thwaites' method to include effects of compressibility.

With the presence of heat transfer the application of Stewartson's transformation does not correlate a given compressible problem to an equivalent incompressible one. Thus, the universal relation previously described is not adequate. Unfortunately, there is little possibility of establishing a family of "universal" relations with, for example, the wall temperature as the distinguishing parameter, since a variety of exact solutions to this problem are not available. However, one such set of relations may be obtained from the solutions of references 11 and 12.

In the present paper, after formulation of a nonlinear system of two first-order differential equations (with the major restriction being a linear viscosity law), methods of solution are developed depending on Thwaites' concept of universal functions. The functions used for this purpose are evaluated from the solutions of reference 12 only.

BOUNDARY-LAYER EQUATIONS

The equations of the steady, two-dimensional compressible laminar boundary layer for perfect fluids are

²Other approaches, such as that of Young and Winterbottom (ref. 21), have resulted in expressions for the momentum thickness similar to that of Thwaites. In that analysis, however, the derivation was a modification of the Pohlhausen technique. The application of a correlation concept was not proposed.

Continuity:

$$\frac{\partial}{\partial x} (\rho u) + \frac{\partial}{\partial y} (\rho v) = 0 \quad (1)$$

Momentum:

$$\left. \begin{aligned} \rho u \frac{\partial u}{\partial x} + \rho v \frac{\partial u}{\partial y} &= - \frac{\partial p}{\partial x} + \frac{\partial}{\partial y} \left(\mu \frac{\partial u}{\partial y} \right) \\ \frac{\partial p}{\partial y} &= 0 \end{aligned} \right\} \quad (2)$$

Energy:

$$\rho u \frac{\partial h}{\partial x} + \rho v \frac{\partial h}{\partial y} = u \frac{\partial p}{\partial x} + \frac{\partial}{\partial y} \left(\frac{\mu}{Pr} \frac{\partial h}{\partial y} \right) + \mu \left(\frac{\partial u}{\partial y} \right)^2 \quad (3)$$

All symbols are defined in appendix A.

The viscosity law to be assumed is

$$\frac{\mu}{\mu_0} = \lambda \frac{t}{t_0} \quad (4)$$

Equation (4) is of the form taken by Chapman and Rubesin (ref. 5), except that the reference conditions (μ_0, t_0) are free-stream stagnation values, since, in the case of pressure gradient, the local "external" values are not constant along the flow. The constant λ is used to match the viscosity with the Sutherland value at a desired location. If this location is assumed to be the surface, the result is

$$\lambda = \left(\frac{t_0 + k_{su}}{t_w + k_{su}} \right) \sqrt{\frac{t_w}{t_0}} \quad (5)$$

where

$$k_{su} = \text{Sutherland's constant} = 216^\circ \text{ R (for air)}$$

Stewartson's transformation. - By using the following definitions of the stream function:

$$\left. \begin{aligned} \psi_y &= \frac{\rho u}{\rho_0} \\ \psi_x &= - \frac{\rho v}{\rho_0} \end{aligned} \right\} \quad (6)$$

a slight modification of Stewartson's transformation (ref. 23) may be written

$$\left. \begin{aligned} dX &= \lambda \frac{a_e}{a_0} \frac{p_e}{p_0} dx \\ dY &= \frac{\rho}{\rho_0} \frac{a_e}{a_0} dy \end{aligned} \right\} \quad (7)$$

The transformed coordinates are now represented by upper-case letters (X, Y), and the subscript e refers to local conditions at the outer edge of the boundary layer (external) where the flow is assumed to be isentropic. The subscript 0 refers to free-stream stagnation values.

Applying equations (4) to (7) to the boundary-layer equations (1) to (3) and assuming that Pr and c_p are constant (but not yet requiring that Pr = 1) result in the following system:

$$U_X + V_Y = 0 \quad (8)$$

$$UU_X + VU_Y = U_e U_{eX} (1 + S) + \nu_0 U_{YY} \quad (9)$$

$$US_X + VS_Y = \nu_0 \left\{ \frac{S_{YY}}{\text{Pr}} - \frac{1 - \text{Pr}}{\text{Pr}} \left(\frac{\frac{\gamma - 1}{2} M_e^2}{1 + \frac{\gamma - 1}{2} M_e^2} \right) \left[\left(\frac{U}{U_e} \right)^2 \right]_{YY} \right\} \quad (10)$$

where the enthalpy term S is defined for convenience as

$$S = \frac{h_s}{h_0} - 1 \quad (11)$$

where h_s is the local stagnation enthalpy, and where the stream function has been replaced by the transformed velocities (U, V) through the relations

$$\begin{aligned} U &\equiv \psi_Y \\ V &\equiv -\psi_X \end{aligned} \quad (12)$$

The resulting relation between the transformed and physical longitudinal velocities is $U = \frac{a_0}{a_e} u$.

The boundary conditions applicable to the system (8), (9), and (10) for a specified wall temperature are

$$\left. \begin{aligned} U(X,0) &= 0 \\ V(X,0) &= 0 \\ S(X,0) &= S_w(X) \\ \lim_{Y \rightarrow \infty} S &= 0 \\ \lim_{Y \rightarrow \infty} U &= U_e(X) \end{aligned} \right\} \quad (13)$$

Integral equations. - An alternate form of the momentum equation may be obtained by subtracting the momentum equation (9) from the product of the continuity equation (8) and the quantity $(U_e - U)$. This results in

$$\left[U(U_e - U) \right]_X + \left[V(U_e - U) \right]_Y + U_{eX}(U_e - U) + U_e U_{eX} S = -\nu_0 U_{YY} \quad (14)$$

If equation (14) is integrated with respect to Y between the limits $Y = 0$ and $Y = \Delta$, where Δ is a constant distance normal to the surface sufficiently large that the conditions $S = 0$ and $U = U_e$ can both be satisfied, there results

$$\frac{d}{dX} (\theta_i U_e^2) + U_e U_{eX} (\delta_i^* + \mathcal{E}) = \nu_0 (U_Y)_{Y=0} \quad (15)$$

where the transformed momentum thickness θ_i , the transformed displacement thickness δ_i^* , and the enthalpy thickness \mathcal{E} , are defined as

$$\left. \begin{aligned} \theta_i &\equiv \int_0^\Delta \frac{U}{U_e} \left(1 - \frac{U}{U_e} \right) dY \\ \delta_i^* &\equiv \int_0^\Delta \left(1 - \frac{U}{U_e} \right) dY \\ \mathcal{E} &\equiv \int_0^\Delta \left(\frac{h_s}{h_0} - 1 \right) dY = \int_0^\Delta S dY \end{aligned} \right\} \quad (16)$$

By carrying out the indicated differentiation, equation (15) can be put in the form

$$\frac{d\theta_i}{dX} + \frac{U_{eX}}{U_e} (2\theta_i + \delta_i^* + \mathcal{E}) = \frac{v_0}{U_e^2} (U_Y)_w \quad (17)$$

This equation has the form of the conventional Kármán momentum integral with the exception of the enthalpy term \mathcal{E} .

It should be noted that because of Stewartson's transformation a simple relation exists between the parameter θ_i and the actual physical momentum thickness θ . This relation is

$$\theta = \frac{p_0}{p_e} \frac{a_e}{a_0} \theta_i = \theta_i \left(\frac{t_0}{t_e} \right)^{\frac{\gamma+1}{2(\gamma-1)}} \quad (18)$$

Following a procedure with the energy equation similar to that for the momentum equation results in

$$\frac{dE}{dX} + \frac{U_{eX}}{U_e} E = - \frac{v_0}{Pr U_e} \left(\frac{\partial S}{\partial Y} \right)_w \quad (19)$$

where the enthalpy-flux thickness is defined by

$$E = \int_0^\Delta S \frac{U}{U_e} dY \quad (20)$$

The method presented in this report uses exact solutions to the boundary-layer equations including the energy equation. Since both the skin-friction and heat-transfer parameters from the exact solutions are correlated with a parameter which is evaluated from only the momentum integral equation, it will not be necessary to use equations (19) and (20).

REDUCED BOUNDARY-LAYER EQUATIONS

At this stage, the relation governing the boundary-layer development is equation (17), subject to the boundary conditions $(\theta_i)_{X=0} = 0$ or $(\theta_i)_{sp}$ where the subscript sp indicates stagnation-point values. The former condition on θ_i applies when the boundary layer is initiated

without a stagnation point (such as in the case of a supersonic thin airfoil). The value of $(\theta_i)_{sp}$ depends on the value of $(U_{ex})_{sp}$ and on the surface temperature. Values of θ_{sp} are presented in table I.

Before consideration of a solution which depends on a correlation similar to that of Thwaites, it is expedient to transform the preceding system of equations to a system involving dimensionless parameters. The correlation concept will then be introduced and methods of solution developed.

Parametric Form

The dimensionless parameters, which are related to terms appearing in equations (17) and (19), can be defined and evaluated from the following expressions:

Shear parameter, or first-derivative parameter,

$$l \equiv \frac{\theta_i}{U_e} \left(\frac{\partial U}{\partial Y} \right)_w = \frac{\theta}{u_e} \frac{t_w}{t_e} \left(\frac{\partial u}{\partial y} \right)_w \quad (21)$$

Correlation number (related to pressure gradient), or second-derivative parameter,

$$n \equiv - \frac{U_{ex}}{v_0} \theta_i^2 = \frac{\theta_i^2}{U_e} \frac{\left(\frac{\partial^2 U}{\partial Y^2} \right)_w}{1 + S_w} = - \frac{u_{ex} \theta^2}{v_w} \left(\frac{t_w}{t_e} \right)^2 \left(\frac{t_0}{t_e} \right) \quad (22)$$

Heat-transfer parameter, or third-derivative parameter,

$$r \equiv \frac{\theta_i^3}{U_e} \left(\frac{\partial^3 U}{\partial Y^3} \right)_w = n \theta \frac{t_w}{t_0} \left[\frac{\partial}{\partial y} \left(\frac{t}{t_e} \right) \right]_w \quad (23)$$

In the definitions (22) and (23), use is made of the following relations, respectively:

$$\left(\frac{\partial^2 U}{\partial Y^2} \right)_w = - \frac{U_e U_{ex}}{v_0} (1 + S_w) \quad (24)$$

which is obtained from equation (9), and

$$\left(\frac{\partial S}{\partial Y}\right)_w = - \frac{v_0}{U_e U_{eX}} \left(\frac{\partial^3 U}{\partial Y^3}\right)_w \quad (25)$$

which is obtained by differentiating equation (9) with respect to Y and evaluating the resulting expression at $Y = 0$.

If equation (17) is multiplied by $\frac{2\theta_i U_e}{v_0}$, there results

$$\frac{U_e}{v_0} \frac{d(\theta_i^2)}{dX} = -2 \left[\frac{U_{eX}}{v_0} \theta_i^2 (H_{inc} + 2) - \frac{\theta_i}{U_e} \left(\frac{\partial U}{\partial Y}\right)_w \right] \quad (26)$$

where $H_{inc} = \frac{\delta_i^* + \mathcal{E}}{\theta_i}$ is the form factor for low-speed flow ($M_e \approx 0$).

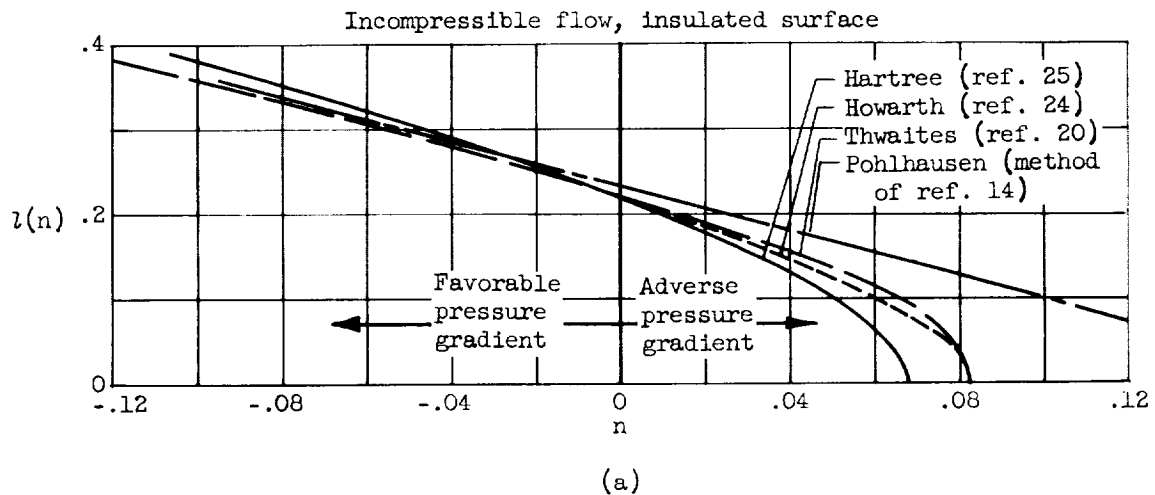
Now, if the definitions (21) and (22) are inserted, equation (26) becomes

$$-U_e \frac{d}{dX} \left(\frac{n}{U_{eX}} \right) = 2 \left[n(H_{inc} + 2) + 1 \right] \quad (27)$$

A similar procedure can be carried out with the energy equation, although it is not necessary for the calculation method herein presented.

Correlation in Terms of n

If, in the definition of H_{inc} (eq.(26)), \mathcal{E} is set equal to zero, equation (26) becomes Thwaites' momentum equation. If, in this case, physically valid relations $H(n)$ and $l(n)$ can be established, the equation can be integrated and the problem is solved. The assumption of the form of the velocity profile serves this purpose, and the resultant procedure is the well-known Pohlhausen technique. (Kalikhman (ref. 15) was the first to carry the same approach over to the case of the thermal profile.) Thwaites used the more direct approach by determining whether universal relations $H(n)$ and $l(n)$ could possibly be established from the well-known "exact" solutions of the boundary-layer problem. An examination of these solutions proved that for favorable pressure gradients a single relation for each of these quantities could be established with a fair degree of accuracy, but for adverse pressure gradients the relations departed from each other considerably, as indicated for $l(n)$ in sketch (a) (taken from ref. 20). Since the correlation technique requires



the selection of a single relation between all boundary-layer quantities regardless of the history of the development of the specific boundary layer under consideration, the assumption of a single relation for all boundary layers is not exactly valid. Thwaites chose a relation for $l(n)$ that would match the Howarth solution (ref. 24) at separation. The Pohlhausen solution predicts separation to occur much later than any of the other solutions in the sketch, while the Hartree solution (ref. 25) predicts separation to occur earlier than the Howarth solution. Stewartson (ref. 23) has indicated that under certain conditions Howarth's solution would predict separation too late.

With the exception of the described differences in the relation between boundary-layer quantities (due to the selection of the solutions of ref. 12 for the evaluation of the correlated quantities), the method of correlation to be presented herein will contain as special cases the method of Thwaites for incompressible flow and the results of Rott and Crabtree for compressible flow over insulated surfaces.

The concept of correlation is herein extended by the following major assumption: For the compressible laminar boundary layer with heat transfer across the surface, the skin-friction and heat-transfer parameters l and r can be correlated only in terms of the parameters n and S_w , derived from the exact solutions of reference 12.

It is thus implied that the solutions of reference 12 adequately represent the general boundary layer, although they were derived for Falkner-Skan type flow.

As in all first-order boundary-layer theories, the pressure distribution (and consequently the external velocity distribution) is assumed

to be known. Then the utility of the correlation may be stated as follows: If n were known at a given point on the surface, θ_i (and hence θ) can immediately be obtained from equation (22). If $l(n)$ is a known function for the specified wall temperature, the wall shear is immediately obtainable from equation (21). Similarly, if $r(n)$ is known, the heat transfer can be found from equation (23).

If the postulate of correlation in terms of n and S_w be admitted, equation (27) becomes

$$- U_e \frac{d}{dX} \left(\frac{n}{U_{eX}} \right) = N(n, S_w) \quad (28)$$

where

$$N(n, S_w) \equiv 2[n(H_{inc} + 2) + l] \quad (29)$$

This is the fundamental equation of the present method. Its solution, resulting in a determination of $n(x)$, is the first stage in solving for the boundary-layer characteristics. Then the function $l(n, S_w)$ is used to determine the wall shear, and the function $r(n, S_w)$ is used to determine the heat transfer.

Evaluation of Correlation Parameters

The quantities l , n , and r defined in equations (21) to (23), as evaluated from the solutions of reference 12, are listed in table II. An alternate parameter to r for the determination of the heat transfer is the Reynolds analogy parameter, defined as $\frac{C_f Re_w}{Nu}$, relating the heat transfer to the skin friction. Because this (arbitrarily chosen) parameter is herein determined from solutions for a Prandtl number of 1.0, it will be denoted $\left(\frac{C_f Re_w}{Nu} \right)_{Pr=1}$ as it appears in table II. It is related to r by

$$\left(\frac{C_f Re_w}{Nu} \right)_{Pr=1} = - \frac{2S_w n l}{r} \quad (30)$$

The parameters l and $\left(\frac{C_f Re_w}{Nu} \right)_{Pr=1}$ as functions of n and S_w are plotted against n in figures 1 and 2, respectively. The solid portions of the curves represent the solutions of reference 12. The reversal of the curves for $S_w = 1.0$ is associated with the velocity overshoot phenomenon discussed in reference 12.

When very strong favorable pressure gradients are maintained for some distance along a surface, it may become necessary to select a correlation for a range of correlation numbers more negative than those resulting from the calculations based on reference 12. This may be illustrated by comparison of the extreme case of a Falkner-Skan type flow having an infinitely favorable pressure gradient ($\beta = 2$) with the case of a real flow having a fixed favorable gradient following a run of zero pressure gradient. In the extreme case it can be shown that the momentum thickness is always zero, but that the correlation number (proportional to $-u_{e_x} \theta^2$) is finite since u_{e_x} is infinite. With the real flow, the momentum thickness in the region of favorable pressure gradient can be made as large as desired by increasing the length of run preceding the favorable gradient. Thus, the value of n may become as negative as desired. Under such circumstances extrapolated correlation functions would have to be used. The broken portions of the curves of figures 1, 2, and 6 represent an extrapolation that is assumed to be qualitatively correct and quantitatively reasonable.

METHOD OF SOLUTION

The solution of equation (28) obviously depends on a knowledge of the term $N(n, S_w)$. This quantity was evaluated from equation (29) and the associated formulas for l , n , and H_{inc} . The results are shown in figure 3. It is to be noted that the curve for $S_w = 0$ is nearly a straight line; and for all negative values of S_w the curves depart only slightly from this condition except in the range near separation where the curves become double-valued. For $S_w > 0$ (hot wall) the curve is essentially straight except in the region of strong favorable gradients.

The examination of these curves and of equation (28) suggests two methods of determining the correlation number n . The first method is that of solving equation (28) by numerical integration. This method is assumed applicable to either variable or constant wall temperature. The necessary numerical procedure, however, is tedious, since it involves integration of a first-order nonlinear nonhomogeneous ordinary differential equation. Because a simpler method is available when the surface is isothermal, no numerical integration procedure will be presented here in detail. However, some integration relations are stated in appendix B.

The second method, applicable when the surface temperature is constant (or, presumably, nearly constant), will be termed the "linear method." This method uses the nearly linear shape of the curves of N against n for constant S_w . It directly corresponds to the procedure of Thwaites for incompressible flow and to that of Rott and Crabtree for compressible flow over insulated surfaces. The curve of N against n for a given S_w is assumed represented by

$$N = A + Bn \quad (31)$$

If equation (31) is inserted in equation (28), a simple linear first-order equation results, which has for its solution

$$n = -AU_e^{-B} U_{eX} \int_0^X U_e^{B-1} dX \quad (32)$$

If equation (32) is transformed to physical quantities by using Stewartson's transformation, there results for two-dimensional flow

$$\frac{n}{P' \frac{t_0}{t_e}} = A \left(\frac{t_e}{t_0} \right)^{-K} M_e^{1-B} \int_0^{\frac{x}{L}} \left(\frac{t_e}{t_0} \right)^K M_e^{B-1} d\left(\frac{x}{L}\right) \quad (33)$$

where $K = \frac{3\gamma-1}{2(\gamma-1)}$, L is any fixed length, and the dimensionless pressure gradient P' is given by

$$P' = \frac{L \frac{dp_e}{dx}}{\rho_e u_e^2} = \frac{L \frac{dp_e}{dx}}{\gamma p_e M_e^2} \quad (34)$$

The left member of equation (33) has been arranged in a form convenient for later use.

The determination of the coefficients A and B is as follows: If the straight line (31) is chosen to pass through the correct value of N at zero pressure gradient ($n = 0$), then $A = 0.44$ independent of S_w . In this case, only B is affected by the presence of heat transfer. Figure 4 shows the values of $B(S_w)$ for the following choices of matching conditions:

(1) The line (31) goes through the point corresponding to $N = 0$ ($u_e = 0$) in order to match the conditions at a stagnation point. Thus, for two-dimensional flow ($N = 0$), $B = -0.44/n_{sp}$.

(2) The line (31) coincides with the tangent to the $N(n)$ lines at $n = 0$ (small pressure gradients).

(3) The line (31) is selected to give good over-all agreement for unfavorable pressure gradients.

If a better match with the curves of figure 3 is desired in calculating n for certain ranges of pressure gradient, a tangent line to the curve of N against n may be chosen at a desired value of n .

For instance, in considering the flow in the vicinity of a two-dimensional stagnation point with $S_w = -0.8$, the tangent line through $N = 0$ has the coefficients $A = 0.372$, $B = 2.53$. The value of B is quite sensitive to the matching assumption, especially in the region $S_w > 0$ (fig. 4). However, the final value of $n(x)$ is somewhat insensitive to the value of B , since the terms involving B in equation (33) appear both inside and outside the integral in a compensating manner. The accuracy of the method decreases, of course, in regions where the plots of figure 3 have large curvature.

The calculation procedure is as follows: Values of A and B are chosen for use in equation (33) either from figure 4 or from tangent-line considerations. The integration is then performed by using a suitable integration rule and a proper step size. It is recommended that the step size chosen be as small as practicable in order to obtain results which are reasonably smooth. In some cases (e.g., near the boundary-layer origin) it may be advisable to perform the integration by obtaining Taylor's series expansions of the integrand in the variable (x/L) . Then the integration can be carried out in closed form, corresponding effectively to zero step size.

There are two possible starting conditions in a boundary-layer calculation: (1) that of a sharp edge, that is, $\theta = 0$, $n = 0$; or (2) the stagnation point, where $U_e = u_e = 0$. In using the linear method, the starting conditions are automatically satisfied when the chosen line (31) goes through the starting point. Thus, if matching condition (1) is used, both possible starting conditions can be satisfied, since the corresponding line (31) passes through the curve from the exact solutions at both $n = 0$ ($N = 0.44$) and, for the two-dimensional flow, at $N = 0$ ($n_{sp} = -0.44/B$). Values of n for stagnation-point flow taken from figure 3 are shown in figure 5.

The corresponding relations and procedure for axially symmetric flow based on Mangler's transformation (ref. 26) are presented in appendix C.

It is sometimes helpful to have an analytical expression for the initial variation of correlation number as a check on the numerical calculations. The initial variation of n with x for the various starting conditions, as represented by the derivative $\left(\frac{dn}{dx}\right)_{x=0}$, is discussed in appendix D.

BOUNDARY-LAYER CHARACTERISTICS

Once the correlation number n is determined as a function of x , it is possible to obtain l and $\left(\frac{C_f Re_w}{Nu}\right)_{Pr=1}$ from figures 1 and 2. Then, the local skin-friction coefficient and heat transfer are easily calculated from the following relations, which apply to both two-dimensional and axially symmetric flows:

From the definitions $C_f \equiv \frac{\tau_w}{\frac{1}{2} \rho_w u_e^2}$, $Re_w = \frac{u_e x}{\nu_w}$, $Nu = \frac{x \left(\frac{\partial t}{\partial y}\right)_w}{t_{a,w} - t_w}$, and from equations (21) and (22), it follows that

$$C_f \sqrt{Re_w} = 2l \sqrt{-\frac{\frac{x}{u_e} \frac{du_e}{dx}}{\frac{t_e}{n} \frac{t_0}{t_e}}} \quad (35)$$

or that (the equivalent form which may be more convenient)

$$C_f \sqrt{Re_w} = 2l \sqrt{\frac{\frac{x}{L} P' \frac{t_0}{t_e}}{n}} \quad (36)$$

Once C_f is determined, the heat transfer may be calculated from curves of the Reynolds analogy parameter against correlation number of figure 2, by using the relation

$$\frac{Nu}{\sqrt{Re_w}} = \frac{C_f \sqrt{Re_w}}{\left(\frac{C_f Re_w}{Nu}\right)_{Pr=1}} \quad (37)$$

In utilizing equations (36) and (37), it is useful to have the initial values of the parameters. These values are listed in table I. It may be noted that, at a stagnation point, equation (36) reduces to

$$C_f \sqrt{Re_w} = \frac{2l}{\sqrt{-n_{sp}}} \quad (38)$$

The calculations thus far have been for $Pr = 1.0$. The effect of Prandtl number on skin friction is small and is therefore usually neglected. It can be seen from table I that, for stagnation-point flow, the maximum difference in the quantity $C_f \sqrt{Re_w}$ between solutions

for $Pr = 1.0$ and $Pr = 0.7$ is about 7 percent. With regard to heat transfer, Tifford and Chu (ref. 27) have found, from solutions with constant fluid properties, that the effect of Prandtl number on heat transfer can be accounted for by multiplying $\left(\frac{Nu}{\sqrt{Re_w}}\right)_{Pr=1}$ by $(Pr)^\alpha$. Values

of α suggested in reference 27 are as follows: For small pressure gradients, $\alpha = 1/3$; for large adverse pressure gradients, $\alpha = 1/4$; and for extreme favorable gradients, $\alpha = 1/2$. Squire (ref. 28) has indicated that $\alpha = 0.4$ is adequate for stagnation-point flows. Recently obtained solutions (as yet unreported) of equations (16) of reference 12 for $\beta = 1$, $Pr = 0.7$, and $Me \rightarrow \infty$ show that this type of correction may be adequate for all compressible boundary-layer calculations.

It should be noted that, in the definition of Nusselt number, the temperature difference in the denominator was assumed to be $(t_{a,w} - t_w)$. Since for $Pr = 1$ the recovery temperature is t_0 , the present calculations (based on those of ref. 12) can give no indication of the adiabatic wall temperature for $Pr \neq 1$. For a first approximation, it may be reasonable to calculate $t_{a,w}$ by using a temperature recovery factor of $(Pr)^{1/2}$. This is the well-known expression for recovery factor for the case of high-speed flow with zero pressure gradient. The accuracy of its application to flows with large pressure gradients is not yet established.

The physical momentum thickness is determined from

$$\frac{\theta}{L} \sqrt{Re_w} = \frac{t_e}{t_w} \sqrt{\frac{n \frac{x}{L}}{P' \frac{t_0}{t_e}}} \quad (39)$$

The displacement thickness δ^* may be calculated by using the following simple expression for the ratio of displacement thickness to momentum thickness:

$$\frac{\delta^*}{\theta} = H_{inc} \left(\frac{t_0}{t_e} \right) + \left(\frac{t_0}{t_e} - 1 \right) \quad (40)$$

In reference 22, this expression was suggested for use in calculating flows over insulated surfaces with $Pr = 1$. For noninsulated surfaces, the dependence of H_{inc} upon wall temperature is presented in figure 6. With large amounts of cooling in favorable pressure gradient flows, it

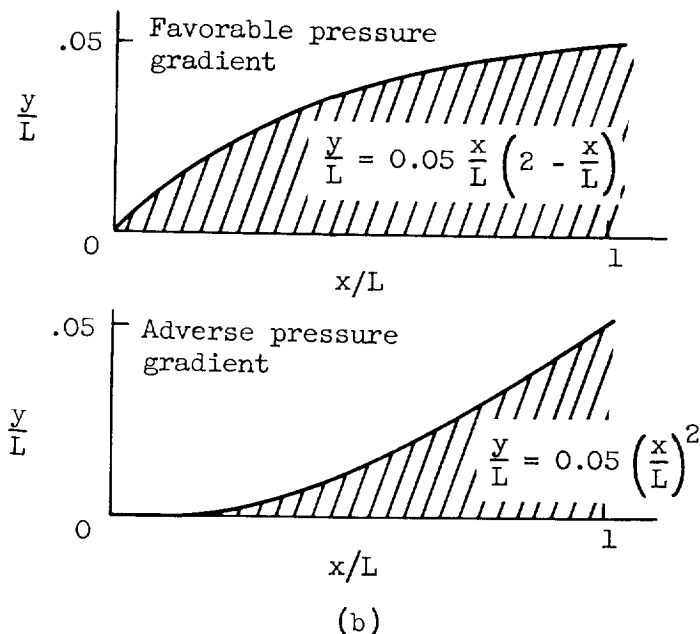
is seen that negative form factors (here corresponding to negative displacement thicknesses) result. This occurs because the surface cooling produces an increase in density near the wall, so that there is more mass flow per unit flow area within the boundary layer than in the external flow.

EXAMPLES

An important test of the method developed is the comparison of the final results for practical problems with the findings of other theories or with experimental results.

I. Supersonic Surfaces

The linear method for determining the correlation number n is applied to the calculation of skin friction and heat transfer for the two supersonic surfaces at Mach number 3.0 calculated in reference 6. These surfaces are shown in sketch (b).



A comparison is made, in the following table, between the results obtained by using the linear method and those obtained by using Low's perturbation method with $Pr = 0.72$ (ref. 6). The comparison is made for a hot wall, an insulated wall, and a cold wall at $x/L = 1$ (see sketch (b)). A value of α of $1/3$ was used in these calculations.

Gradient	Heat-transfer condition	$(C_f \sqrt{Re_w})_{x/L=1}$		$(Nu/\sqrt{Re_w})_{x/L=1}$	
		Linear method, Pr = 1	Low (ref. 6), Pr = 0.72	Linear method, corrected for Pr	Low (ref. 6), Pr = 0.72
Favorable	Cold wall ($S_w = -0.9$)	0.680	0.679	0.270	0.271
	Insulated wall	.877	.876	-----	-----
	Hot wall ($S_w = 0.61$)	1.031	1.048	.284	.318
Adverse	Cold wall ($S_w = -0.9$)	0.645	0.661	0.320	0.307
	Insulated wall	.406	.475	-----	-----
	Hot wall ($S_w = 0.43$)	.256	.386	.274	.277

A comparison of values indicates agreement of skin friction within 2 percent in the case of a favorable pressure gradient. For the adverse pressure gradient cases, reasonable agreement is obtained for the cold wall, although for the insulated and hot walls, a large difference is obtained. This difference is due essentially to the fact that, in the case of an adverse pressure gradient, the solutions of Low (ref. 6), which resemble the series-type solution of Howarth (ref. 24), depart from Falkner-Skan type solutions such as that of Hartree (ref. 25) (e.g., sketch (a)). Some of the difference in the preceding table is a Prandtl number effect; however, for the heated surface with an adverse pressure gradient, the flow is closer to separation than appears permissible for a theory based on small pressure gradients such as that of reference 6; therefore, for this case the present calculation may be more reliable. Good agreement is also obtained for heat transfer except for the case of the heated surface with favorable pressure gradient. Some of that difference might be a Prandtl number effect.

II. Axially Symmetric Convergent-Divergent Rocket Nozzle

The second example, that of a rocket nozzle, is one involving both large pressure gradients and heat transfer. The nozzle chosen is illustrated in figure 7. It has a 25° half-angle convergent section and a 15° half-angle divergent section. The combustion-chamber stagnation

pressure is assumed to be 500 pounds per square inch absolute, the stagnation temperature is taken as 4000° R, and the Prandtl number is assumed to be 0.78. The nozzle wall is assumed cooled to a uniform temperature of 800° R, which corresponds to $S_w = -0.8$. For the assumed 3-inch throat diameter, the rocket has a nominal thrust of 5550 pounds for $\gamma = 1.3$. Local static conditions along the nozzle wall were obtained using one-dimensional flow relations.

The calculation was performed by the linear method with $A = 0.572$ and $B = 2.53$. In order to eliminate the effect of step size in the initial portion of the integration, a series expansion of the integrand was used for $0 \leq (x/L) < 0.5$. For $(x/L) > 0.5$, the step size taken was 0.1. The resulting variation of n in the nozzle is also shown in figure 7. It is seen that, in a portion of the nozzle including the throat ($1.2 < (x/D) < 3.5$), values of n are obtained which are more negative than those obtainable from the exact solutions. Thus, in order to calculate skin friction, heat transfer, and displacement thickness from $1.2 < (x/D) < 3.5$, it is necessary to use the extrapolated portions of the curves of figures 1 and 2 for $S_w = -0.8$. No extrapolation is needed to obtain momentum thickness since the momentum thickness is related to n through equation (39).

The calculated local heat-transfer rates as well as displacement and momentum thickness are shown in figure 8. It is seen that large rates of cooling are required in the neighborhood of the stagnation point and the nozzle throat. If the cooling were to become insufficient, these seem to be the most likely locations of failure. The required local cooling rate to maintain constant wall temperature decreases sharply beyond the throat of the nozzle.

In the absence of more appropriate information, it has been customary in recent years to use flat-plate heat-transfer relations in estimating heat transfer in a nozzle. The use of such a relation in the current problem ($Nu/\sqrt{Re_w} = 0.305$ for $Pr = 0.78$) yields values indicated by the dashed line in figure 8. It is seen that for this problem the flat-plate relation seriously underestimates the amount of cooling required over a large part of the nozzle. This illustrates the importance of considering the effects of pressure gradient on heat transfer.

The momentum thickness is seen to reach a minimum value at the nozzle throat. The displacement thickness is a small positive quantity

3321
CN-3 back

at the stagnation point but is negative for most of the convergent section as well as in the vicinity of the throat.³

The use of different values of A and B in performing the numerical integration would have approximately the following effect: With the values $A = 0.44$ and $B = 3.0$ (from fig. 4), the momentum thickness would be about 10 percent smaller in the vicinity of the throat than the values in figure 7 and would be within 5 percent of the presented values over the rest of the nozzle. With $A = 0.335$ and $B = 2.34$, the momentum thickness at the throat would be about 6 percent larger than the value presented. The effects of varying A and B on skin friction and heat transfer would be less than 3 percent at the throat.

CONCLUDING REMARKS

The application of Stewartson's transformation to the compressible laminar boundary-layer equations with heat transfer yielded a simple first-order system of ordinary differential equations, the first of which is very similar to the Kármán momentum integral. Dimensionless shear and heat-transfer parameters were defined. The assumption of correlation of these parameters in terms of a momentum parameter resulted in a complete system of relations for calculating skin friction and heat transfer. Knowledge of velocity or temperature profiles is not necessary in using this calculation method. Procedures for the calculation of the longitudinal distribution of correlation number are presented, which include as special cases the method of Thwaites and that of Rott and Crabtree. The dimensionless parameters introduced herein were evaluated from the exact solutions of reference 12.

Calculations of an example involving small pressure gradients show that the method is reliable when compared with the perturbation method of reference 6 over the same range of Mach number, pressure gradient, and heat transfer.

The method is also applied to the calculation of heat transfer and displacement thickness in a highly cooled, convergent-divergent, axially symmetric rocket nozzle. The results of this calculation show that high rates of heat transfer are obtained at the initial stagnation point and

³This unusual result produces the interesting possibility that, for a rocket nozzle with cooled walls and viscous flow, a mass discharge coefficient based on throat area, generally assumed to be less than unity because of boundary-layer "blockage" at the throat, may actually exceed 1. A distinction exists between this phenomenon and that of negative momentum thickness (refs. 1, 10, and 12) associated with "velocity overshoot."

at the throat of the nozzle. Also indicated are negative displacement thicknesses in the convergent portion of the nozzle; these occur because of the high density within the lower portions of the cooled boundary layer.

Lewis Flight Propulsion Laboratory
National Advisory Committee for Aeronautics
Cleveland, Ohio, February 1, 1955

APPENDIX A

SYMBOLS

The following symbols are used in this report:

A	constant from $N = A + Bn$
a	sonic velocity
B	constant from $N = A + Bn$
C_f	local skin-friction coefficient, $C_f = \frac{2\tau_w}{\rho_w u_e^2}$
c_p	specific heat at constant pressure
D	nozzle-throat diameter
E	enthalpy-flux thickness, $E = \int_0^\Delta S \frac{U}{U_e} dY$
δ	stagnation-enthalpy-defect thickness, $\delta = \int_0^\Delta \left(\frac{h_s}{h_0} - 1 \right) dY$
H	form factor, $H = \delta^*/\theta$
H_{inc}	physical form factor for $M_e = 0$, $H_{inc} = \frac{\delta_1^* + \delta}{\theta_1}$
h	enthalpy
K	$\frac{3\gamma - 1}{2(\gamma - 1)}$
k	thermal conductivity
k_{su}	Sutherland's constant
L	arbitrary length
l	dimensionless shear parameter, $l = \frac{\theta_1}{U_e} \left(\frac{\partial U}{\partial Y} \right)_w$

M Mach number

m exponent from Falkner-Skan external velocity distribution
 $U_e = CX^m$

N momentum parameter, $N = 2 \left[n(H_{inc} + 2) + 1 \right]$

Nu Nusselt number, $Nu = \frac{x \left(\frac{\partial t}{\partial y} \right)_w}{t_{a,w} - t_w}$

n correlation number, $n = - \frac{U_e \theta_1^2}{v_0}$

P' dimensionless pressure gradient, $P' = \frac{L}{\gamma p_e M_e^2} \frac{dp_e}{dx}$

Pr Prandtl number, $Pr = \frac{\mu c_p}{k}$

p static pressure

q local heat-transfer rate, Btu/(sq ft)(sec)

R radius of axially symmetric body

Re_w Reynolds number, $Re_w = \frac{\rho_w u_e x}{\mu_w}$

r heat-transfer parameter, $r = n\theta \frac{t_w}{t_0} \left[\frac{\partial}{\partial y} \left(\frac{t}{t_e} \right) \right]_w$

S enthalpy function, $S = \frac{h_s}{h_0} - 1$

t static temperature

t_{a,w} adiabatic wall temperature

U	transformed longitudinal velocity, $U = u \frac{a_0}{a_e} = \psi_Y$
u	longitudinal velocity component
V	transformed normal velocity, $V = -\psi_X$
v	normal velocity component
X	transformed coordinate along surface, $X = \int_0^x \lambda \frac{p_e}{p_0} \frac{a_e}{a_0} dx$
x	coordinate along surface
Y	transformed normal coordinate, $Y = \int_0^y \frac{\rho a_e}{\rho_0 a_0} dy$
y	normal coordinate
α	exponent of Prandtl number in Reynolds analogy parameter
β	pressure gradient parameter, $\beta = \frac{2m}{m+1}$
γ	ratio of specific heats
δ^*	displacement thickness
θ	momentum thickness
λ	$\lambda = \frac{(\mu/\mu_0)}{(t/t_0)} = \left(\frac{t_0 + k_{su}}{t_w + k_{su}} \right) \sqrt{\frac{t_w}{t_0}}$
μ	dynamic viscosity
ν	kinematic viscosity, $\nu = \mu/\rho$
ρ	mass density
τ	shear stress, $\tau = \mu \frac{\partial u}{\partial y}$
ψ	stream function, eq. (6)

Subscripts:

- e local flow outside boundary layer (external)
- i associated transformed quantity
- s local stagnation value
- sp stagnation point
- w wall or surface value
- 0 free-stream stagnation value
- 1 initial value

3321

CN-4

APPENDIX B

NUMERICAL INTEGRATION METHOD

Method. - The most direct method of solving equation (28) is by numerical integration, using the calculated curves of $N(n, S_w)$ for determination of the right member. This method is assumed applicable to either variable or constant S_w .

An integration procedure may be simply indicated by direct integration of equation (28). The resultant integral equation can be written:

For two-dimensional flow,

$$n = \frac{U_{eX}}{(U_{eX})_1} \left[n_1 - (U_{eX})_1 \int_0^X \frac{N(n)}{U_e} dX \right] \quad (B1)$$

For an axially symmetric closed body, through Mangler's transformation (ref. 26),

$$n = - \frac{U_{eX}}{R^2} \int_0^X \frac{NR^2}{U_e} dX \quad (B2)$$

Since the integrands contain $N(n)$, which is unknown at this point, no simple evaluation is possible. In fact, these equations are actually only a condensed notation of the procedure to be followed. The integration must be carried out piecemeal, alternating with determination of the left member of the equation and iterating for accuracy.

The necessity of working with the transformed coordinates can be eliminated by considering the Stewartson transformation from U_e to u_e . For example, in physical coordinates equation (B2) becomes

$$\frac{n}{P' \frac{t_0}{t_e}} = \frac{\left(M_e \frac{a_0}{a_e} \frac{p_0}{p_e} \right)}{R^2} \int_0^{\frac{x}{L}} \frac{NR^2 d\left(\frac{x}{L}\right)}{\left(M_e \frac{a_0}{a_e} \frac{p_0}{p_e} \right)} \quad (B2a)$$

where L is any fixed length, and the dimensionless pressure gradient P' is given by

$$P' = \frac{L \frac{dp_e}{dx}}{\rho_e u_e^2} = \frac{L \frac{dp_e}{dx}}{\gamma p_e M_e^2} \quad (B3)$$

If the isentropic relation $p/\rho^\gamma = \text{constant}$ is used in equations (31) and (32) and if the Stewartson transformation is applied, there results:

For two-dimensional flow,

$$\frac{n}{P' \frac{t_0}{t_e}} = M_e \left(\frac{t_0}{t_e} \right)^K \left\{ \int_0^{\frac{x}{L}} \frac{N d\left(\frac{x}{L}\right)}{M_e \left(\frac{t_0}{t_e} \right)^K} - \frac{n_1}{\left[\frac{dM_e}{d\left(\frac{x}{L}\right)} \right]_1} \right\} \quad (B4)$$

For an axially symmetric flow (closed body),

$$\frac{n}{P' \frac{t_0}{t_e}} = \frac{M_e}{R^2} \left(\frac{t_0}{t_e} \right)^K \int_0^{\frac{x}{L}} \frac{NR^2 d\left(\frac{x}{L}\right)}{M_e \left(\frac{t_0}{t_e} \right)^K} \quad (B5)$$

where $K = \frac{3\gamma-1}{2(\gamma-1)}$.

Initial values. - When the numerical integration method is used, certain considerations are necessary in order to start the solution properly. There are two possible starting conditions: (1) sharp edge or pointed body, where $\theta = 0$ and $n = 0$, and (2) stagnation point, where $U_e = u_e = 0$.

In the case of a boundary layer starting from a stagnation point, the initial value n_1 of n is determined from the condition $U_e = 0$, $U_{eX} = \text{constant}$ in equation (28). For two-dimensional stagnation-point flow, the Hartree pressure gradient parameter β is equal to 1.0.

Since, for the Falkner-Skan type flow considered, $N = \frac{2(\beta-1)}{\beta} n$, it is seen that $N = 0$ at a two-dimensional stagnation point. This fixes n at the values shown in figure 5, which were obtained from figure 3. For axially symmetric stagnation-point flow over a closed body, $\beta = 1/2$ (ref. 29), so that $N_1 = -2n_1$. The values of n_1 for axially symmetric stagnation-point flow over a closed body as obtained from figure 3 are also shown in figure 5. For the stagnation-point flow over the blunt lip of an open axially symmetric body, n_{sp} can be shown to have the two-dimensional value.

APPENDIX C

LINEAR METHOD FOR AXIALLY SYMMETRIC FLOW

For axially symmetric flows, the following equation, which is equivalent to equation (33), is obtained by application of the transformation of Mangler (ref. 26):

$$\frac{n}{P' \frac{t_0}{t_e}} = A \left(\frac{t_e}{t_0} \right)^{-K} \frac{M_e^{1-B}}{R^2} \int_0^{\frac{x}{L}} \left(\frac{t_e}{t_0} \right)^K \frac{R^2}{M_e^{1-B}} d\left(\frac{x}{L}\right) \quad (C1)$$

where $R = R(x)$ is the radius of the body at station x , $K = \frac{3\gamma-1}{2(\gamma-1)}$, and

$$P' = \frac{L \frac{dp_e}{dx}}{\gamma p_e M_e^2}$$

In evaluating the coefficients A and B of the straight line

$$N = A + Bn \quad (31)$$

A may be chosen as 0.44 so that the line (31) passes through the correct value of N at $n = 0$. The choice of B may be made so that the line (31) goes through the point where $N = -2n$ in order to match the conditions at an axially symmetric stagnation point. Thus, $B = -\left(\frac{0.44}{n_{sp}} + 2\right)$.

For achieving better agreement with the curves of figure 3 in certain ranges of pressure gradient, a tangent line to the curve of N against n may be chosen as was indicated for two-dimensional flow.

The three possible starting conditions are: (1) For a pointed body, $\theta = 0$, $n = 0$. (2) For a stagnation point on a closed body, $U_e = u_e = 0$ so that $N = -2n$. Values of n_{sp} for this axially symmetric stagnation point are shown in figure 5 and indicated in table II for $\beta = 1/2$. (3) For a stagnation point on the blunt lip of an open axially symmetric body, it can be shown using the axially symmetric form of equation (28) that $N = 0$ so that n_{sp} is that for two-dimensional flow.

APPENDIX D

INITIAL VARIATION OF CORRELATION NUMBER

It is sometimes helpful to have an analytical expression for the initial variation of correlation number as a check on the numerical calculations. The following expressions for $\left(\frac{dn}{dx}\right)_{x=0}$ are determined from equation (28).

Two-Dimensional Flow

Sharp edge:

$$\left(\frac{dn}{dx}\right)_{x=0} = -0.44 \frac{u_{e,x}}{u_e} \left(\frac{t_0}{t_e}\right) \quad (D1)$$

Stagnation point (blunt body):

$$\left(\frac{dn}{dx}\right)_{x=0} = \frac{n_{sp}}{1 + \left(\frac{dN}{dn}\right)_{sp}} \left(\frac{u_{e,xx}}{u_{e,x}}\right)_{sp} \quad (D2)$$

Axially Symmetric Flow

For axially symmetric flow the initial derivatives must be evaluated from the following equation:

$$-\frac{U_e}{R^2} \frac{d}{dX} \left(\frac{nR^2}{U_{e,X}} \right) = N(n, S_w) \quad (D3)$$

Closed Body

Pointed nose:

$$\left(\frac{dn}{dx}\right)_{x=0} = -0.147 \frac{u_{e,x}}{u_e} \left(\frac{t_0}{t_e}\right) \quad (D4)$$

Stagnation point (blunt nose):

$$\left(\frac{dn}{dx}\right)_{x=0} = \frac{n_{sp}}{1 + \left(\frac{dN}{dn}\right)_{sp}} \left[2 \left(\frac{u_{e_{xx}}}{u_{e_x}} \right)_{sp} - \left(\frac{R_{xx}}{R_x} \right)_{sp} \right] \quad (D5)$$

Open Body

Sharp lip:

$$\left(\frac{dn}{dx}\right)_{x=0} = -0.44 \frac{u_{e_x}}{u_e} \left(\frac{t_0}{t_e} \right) \quad (D6)$$

Stagnation point (blunt lip):

$$\left(\frac{dn}{dx}\right)_{x=0} = \frac{n_{sp}}{1 + \left(\frac{dN}{dn}\right)_{sp}} \left[\left(\frac{u_{e_{xx}}}{u_{e_x}} \right)_{sp} - 2 \left(\frac{R_x}{R} \right)_{sp} \right] \quad (D7)$$

REFERENCES

1. Cohen, Clarence B.: Similar Solutions for the Laminar Compressible Boundary Layer with Heat Transfer and Pressure Gradient, and Application to Integral Methods. Ph.D. Thesis, Princeton Univ., 1954.
2. Sternberg, Joseph: A Free-Flight Investigation of the Possibility of High Reynolds Number Supersonic Laminar Boundary Layers. Jour. Aero. Sci., vol. 19, no. 11, Nov. 1952, pp. 721-733.
3. Lees, Lester, and Lin, Chia Chiao: Investigation of the Stability of the Laminar Boundary Layer in a Compressible Fluid. NACA TN 1115, 1946.
4. Crocco, Luigi: The Laminar Boundary Layer in Gases. Rep. CF-1038, Aerophysics Lab., North American Aviation, Inc., July 15, 1948.
5. Chapman, Dean R., and Rubesin, Morris W.: Temperature and Velocity Profiles in the Compressible Laminar Boundary Layer with Arbitrary Distribution of Surface Temperature. Jour. Aero. Sci., vol. 16, no. 9, Sept. 1949, pp. 547-565.
6. Low, George M.: The Compressible Laminar Boundary Layer with Heat Transfer and Small Pressure Gradient. NACA TN 3028, 1953.

7. Tani, Itiro: Further Studies of the Laminar Boundary Layer in Compressible Fluids. Rep. of Aero. Res. Inst., vols. 22-23, no. 322, Tôkyô Imperial Univ., Dec. 1944.
8. Tifford, Arthur N.: The Thermodynamics of the Laminar Boundary Layer of a Heated Body in a High-Speed Gas Flow Field. Jour. Aero. Sci., vol. 12, no. 2, Apr. 1945, pp. 241-251.
9. Levy, Solomon: Heat Transfer to Constant-Property Laminar Boundary-Layer Flows with Power-Function Free-Stream Velocity and Wall-Temperature Variation. Jour. Aero. Sci., vol. 19, no. 5, May 1952, pp. 341-348.
10. Brown, W. Bryon, and Donoughe, Patrick L.: Tables of Exact Laminar-Boundary-Layer Solutions When the Wall is Porous and the Fluid Properties are Variable. NACA TN 2479, 1951.
11. Levy, Solomon: Effect of Large Temperature Changes (Including Viscous Heating) upon Laminar Boundary Layers with Variable Free-Stream Velocity. Jour. Aero. Sci., vol. 21, no. 7, July 1954, pp. 459-474.
12. Cohen, Clarence B., and Reshotko, Eli: Similar Solutions for the Compressible Laminar Boundary Layer with Heat Transfer and Pressure Gradient. NACA TN 3325, 1955.
13. von Kármán, Th.: Über laminare und turbulente Reibung. Z.a.M.M., Bd. 1, Heft. 4, Aug. 1921, pp. 233-252.
14. Pohlhausen, K.: Zur näherungsweise Integration der Differentialgleichung der laminaren Grenzschicht. Z.a.M.M., Bd. 1, Heft 4, Aug. 1921, pp. 252-268.
15. Kalikhman, L. E.: Heat Transmission in the Boundary Layer. NACA TM 1229, 1949.
16. Ginzler, I.: Ein Pohlhausenverfahren zur Berechnung laminarer kompressibler Grenzschichten an einer geheizten Wand. Z.a.M.M., Bd. 29, Heft 11/12, Nov./Dec. 1949, pp. 321-337.
17. Morris, Deane N., and Smith, John W.: The Compressible Laminar Boundary Layer with Arbitrary Pressure and Surface Temperature Gradients. Jour. Aero. Sci., vol. 20, no. 12, Dec. 1953, pp. 805-818.
18. Libby, Paul A., and Morduchow, Morris: Method for Calculation of Compressible Laminar Boundary Layer with Axial Pressure Gradient and Heat Transfer. NACA TN 3157, 1954.

19. Beckwith, Ivan E.: Heat Transfer and Skin Friction by an Integral Method in the Compressible Laminar Boundary Layer with a Stream-wise Pressure Gradient. NACA TN 3005, 1953.
20. Thwaites, B.: Approximate Calculation of the Laminar Boundary Layer. Aero. Quarterly, vol. 1, Nov. 1949, pp. 245-280.
21. Young, A. D., and Winterbottom, N. E.: Note on the Effect of Compressibility on the Profile Drag of Aerofoils at Subsonic Mach Numbers in the Absence of Shock Waves. R. & M. No. 2400, British A.R.C., May 1940.
22. Rott, Nicholas, and Crabtree, L. F.: Simplified Laminar Boundary-Layer Calculations for Bodies of Revolution and for Yawed Wings. Jour. Aero. Sci., vol. 19, no. 8, Aug. 1952, pp. 553-565.
23. Stewartson, K.: Correlated Incompressible and Compressible Boundary Layers. Proc. Royal Soc. (London), ser. A, vol. 200, no. A1060, Dec. 22, 1949, pp. 84-100.
24. Howarth, L.: On the Solution of the Laminar Boundary Layer Equations. Proc. Roy. Soc. (London), ser. A, vol. 164, no. A919, Feb. 1938, pp. 547-579.
25. Hartree, D. R.: On an Equation Occurring in Falkner and Skan's Approximate Treatment of the Equations of the Boundary Layer. Proc. Cambridge Phil. Soc., vol. 33, pt.2, Apr. 1937, pp. 223-239.
26. Mangler, W.: Compressible Boundary Layers on Bodies of Revolution. VG83, No. 47T, M.A.P. Volkenrode.
27. Tifford, Arthur N., and Chu, S. T.: Heat Transfer in Laminar Boundary Layers Subject to Surface Pressure and Temperature Distributions. Proc. Second Midwestern Conf. on Fluid Mech., Ohio State Univ., Mar. 17-19, 1952, pp. 363-377.
28. Goldstein, Sydney, ed.: Modern Developments in Fluid Dynamics. Vol. 2. Clarendon Press (Oxford), 1938, pp. 631-632.
29. Schlichting, Herman: Grenzschicht-Theorie. Verlag und Druck G. Braun, Karlsruhe, 1951, pp. 110-115.

3321

CN-5

TABLE I. - INITIAL VALUES OF PARAMETERS

(a) Stagnation-point flow

S_w	$C_f \sqrt{Re_w}$		$Nu / \sqrt{Re_w}$			$\delta_{sp}^* \sqrt{\frac{u_{ex}}{v_w}} \left(\frac{t_w}{t_0} \right)$	$\theta_{sp} \sqrt{\frac{u_{ex}}{v_w}} \left(\frac{t_w}{t_0} \right)$	H_{sp}'
	Pr = 1	Pr = 0.7 (a)	Pr = 1	Pr = 0.7 (b)	Pr = 0.7 (a)	Pr = 1	Pr = 1	Pr = 1
Two-dimensional ($\beta = 1$)								
-1.0	^c 1.30	1.21	^c 0.506	0.438	0.436	^c -0.170	^c 0.400	^c -0.425
-0.8	^c 1.56	1.49	^c .522	.452	.451	^c .012	^c .384	^c .031
-0.4	^c 2.04	2.00	^c .546	.474	.475	^c .345	^c .338	^c 1.021
0	2.46	2.46	.570	.495	.495	.648	.292	2.218
1.0	3.47	3.54	.615	.533	.537	1.386	.177	7.850
Axially symmetric ($\beta = 1/2$)								
-1.0	1.64	1.56	0.700	0.607	0.607	-0.0771	0.300	-0.257
-0.8	1.85	1.79	.712	.617	.621	.0576	.289	.199
-0.4	2.25	2.22	.739	.639	.643	.318	.269	1.185
0	2.62	2.62	.763	.662	.662	.569	.248	2.298
1.0	3.49	3.55	.809	.701	.708	1.165	.194	6.012

^aThese values are obtained when eqs. (16) of ref. 12 are solved for Pr = 0.7, $Me = 0$.^bThese values are obtained by multiplying the results for Pr = 1 by $(0.7)^{0.4}$.^cInterpolated values from solutions of ref. 12.

(b) Sharp edge or pointed body

$C_f \sqrt{Re_w}$	$Nu / \sqrt{Re_w}$	
	Pr = 1	Pr = 0.7 (a)
Two-dimensional		
0.664	0.332	0.295
Axially symmetric		
1.150	0.575	0.510

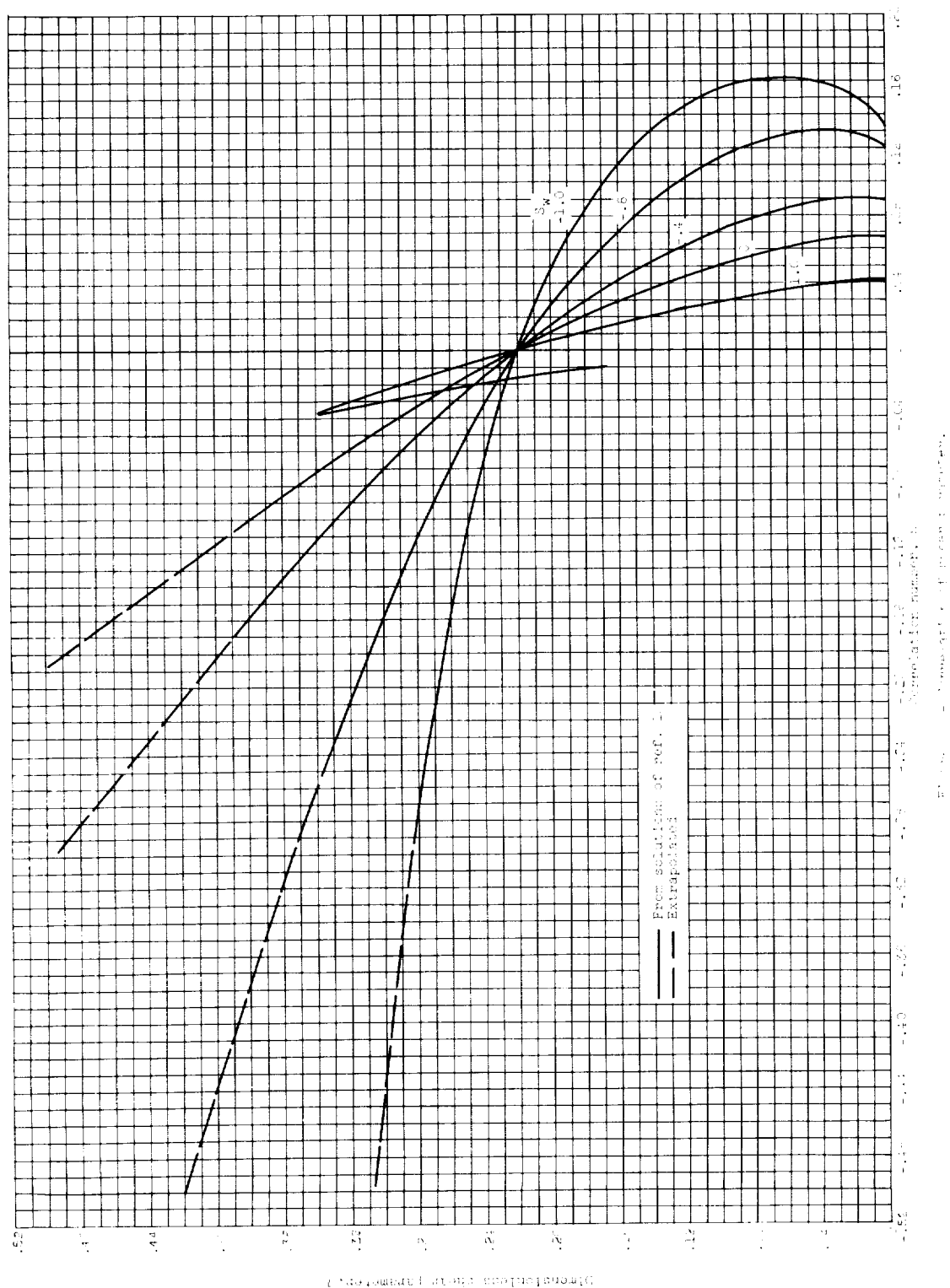
^aThese values are obtained by multiplying the results for Pr = 1 by $(0.7)^{1/3}$.

TABLE II. - SUMMARY OF HEAT-TRANSFER AND WALL-SHEAR PARAMETERS

S_w	β	n	l	N	r	$\left(\frac{C_f Re_w}{Nu}\right)_{Pr=1}$	H_{inc}
-1.0	-0.326	0.1335	0	1.0845	0.0212	0	2.063
	-.3657	.1579	.3929	1.1804	.0307	.3381	1.530
	-.3884	.1591	.0896	1.1382	.0359	.7939	1.013
	-.360	.1257	.1446	.9504	.0297	1.224	.630
	-.30	.0907	.1749	.7858	.0212	1.493	.404
	-.14	.0343	.2063	.5590	.00774	1.830	.134
	0	0	.220	.440	0	2.000	0
	.50	-.0897	.2459	.1793	-.0188	2.347	-.257
	2.00	-.2938	.2829	-.2933	-.0586	2.837	-.538
-0.8	-0.3088	0.1215	0	1.0305	0.0172	0	2.240
	-.325	.1304	.0312	1.0606	.0210	.3100	1.828
	-.3285	.1298	.0436	1.0499	.0216	.4194	1.708
	-.3285	.1260	.0681	1.0185	.0220	.6245	1.501
	-.325	.1212	.0827	.9885	.0216	.7438	1.396
	-.30	.1017	.1214	.882	.0187	1.058	1.138
	-.14	.0355	.1935	.5781	.00642	1.712	.692
	0	0	.220	.44	0	2.000	.518
	.50	-.0837	.2678	.1676	-.0138	2.599	.199
	1.50	-.2008	.3179	-.1332	-.0313	3.263	-.083
	2.00	-.2522	.3366	-.2517	-.0388	3.502	-.166
-0.4	-0.246	0.0899	0	0.9087	0.00679	0	3.041
	-.2483	.0894	.0300	.8968	.00730	.2941	2.679
	-.24	.0826	.0624	.8519	.00696	.5775	2.399
	-.20	.0615	.1210	.7379	.00554	1.074	2.034
	0	0	.220	.440	0	2.000	1.555
	.50	-.0722	.3019	.1442	-.00573	3.042	1.185
	2.00	-.1733	.3924	-.1713	-.0118	4.628	.759
0	-0.1988	0.0681	0	0.822	0	0	4.032
	-.16	.0487	.1051	.7068	0	.9480	3.094
	0	0	.220	.440	0	2.000	2.602
	.50	-.0602	.3220	.1232	0	3.436	2.298
	1.00	-.0829	.3556	0	0	4.317	2.218
	1.60	-.1002	.3808	-.0748	0	5.122	2.180
	2.00	-.1064	.3892	-.1040	0	5.665	2.152
1.0	-0.1295	0.0417	0	0.7280	-0.00803	0	6.723
	-.10	.0294	.09798	.6476	-.00644	.8956	5.671
	0	0	.220	.440	0	2.000	5.183
	.30	-.0334	.3277	.1558	.00607	3.602	5.493
	.50	-.0375	.3384	.0755	.00588	4.315	6.012
	1.00	-.0312	.3065	0	.00338	5.644	7.850
	1.50	-.0186	.2382	-.0114	.00133	6.662	11.125
	2.00	-.0089	.1663	-.0088	.00034	7.527	17.105

3321

CN-5 back



3321

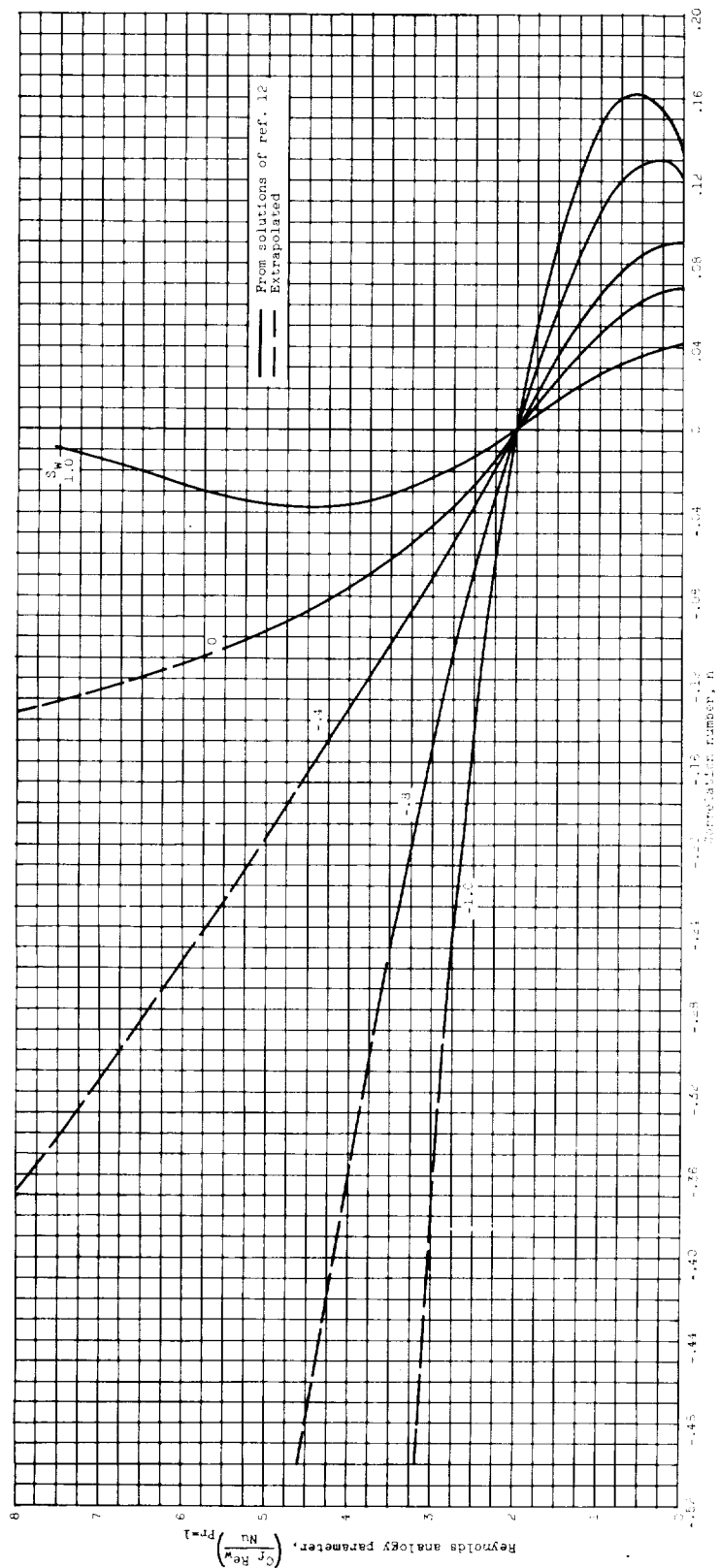


Figure 2. - Correlation of Reynolds analogy parameter.

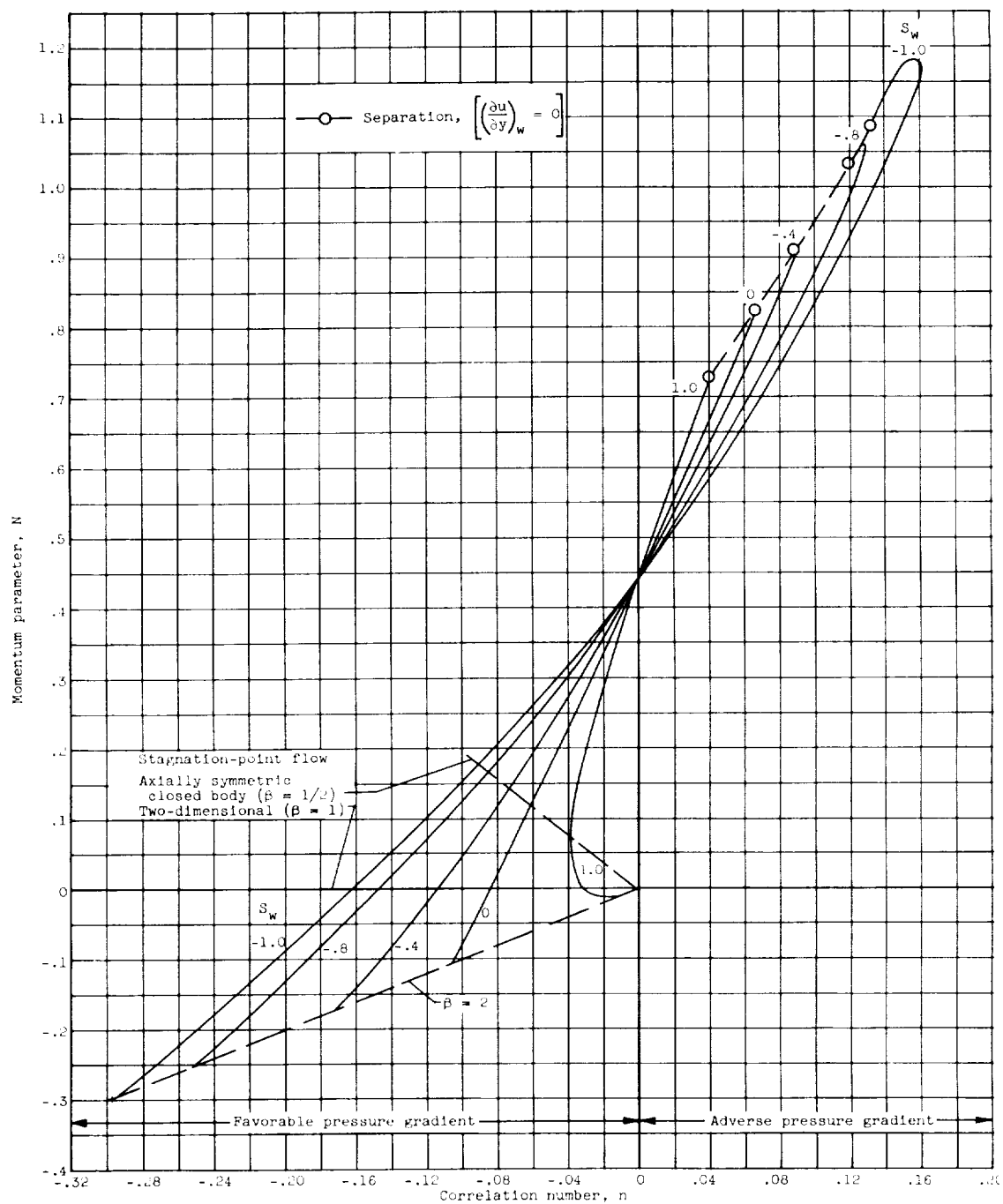


Figure 3. - Correlation of dimensionless momentum equation.

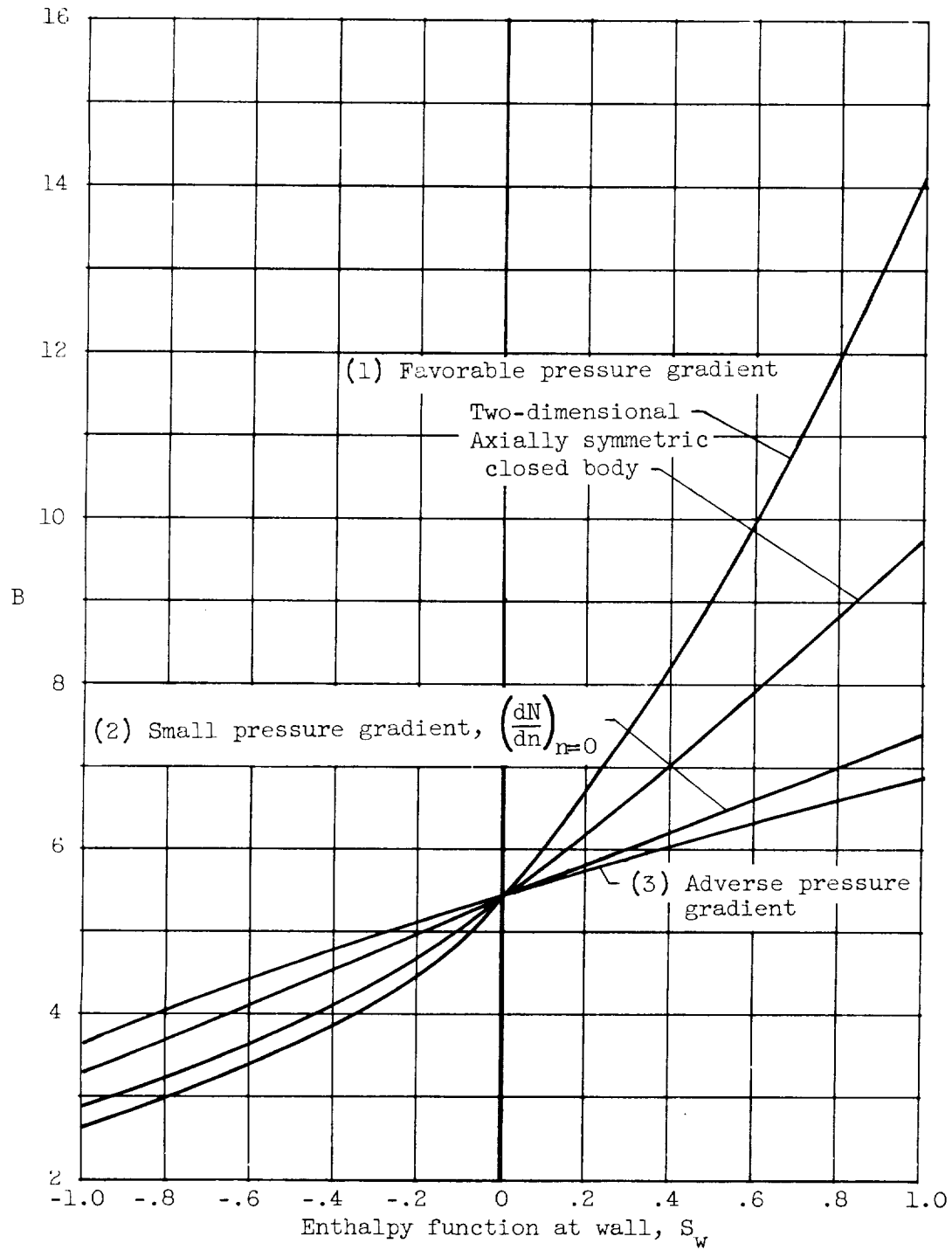


Figure 4. - Variation of B for use in linear method of determining correlation number.

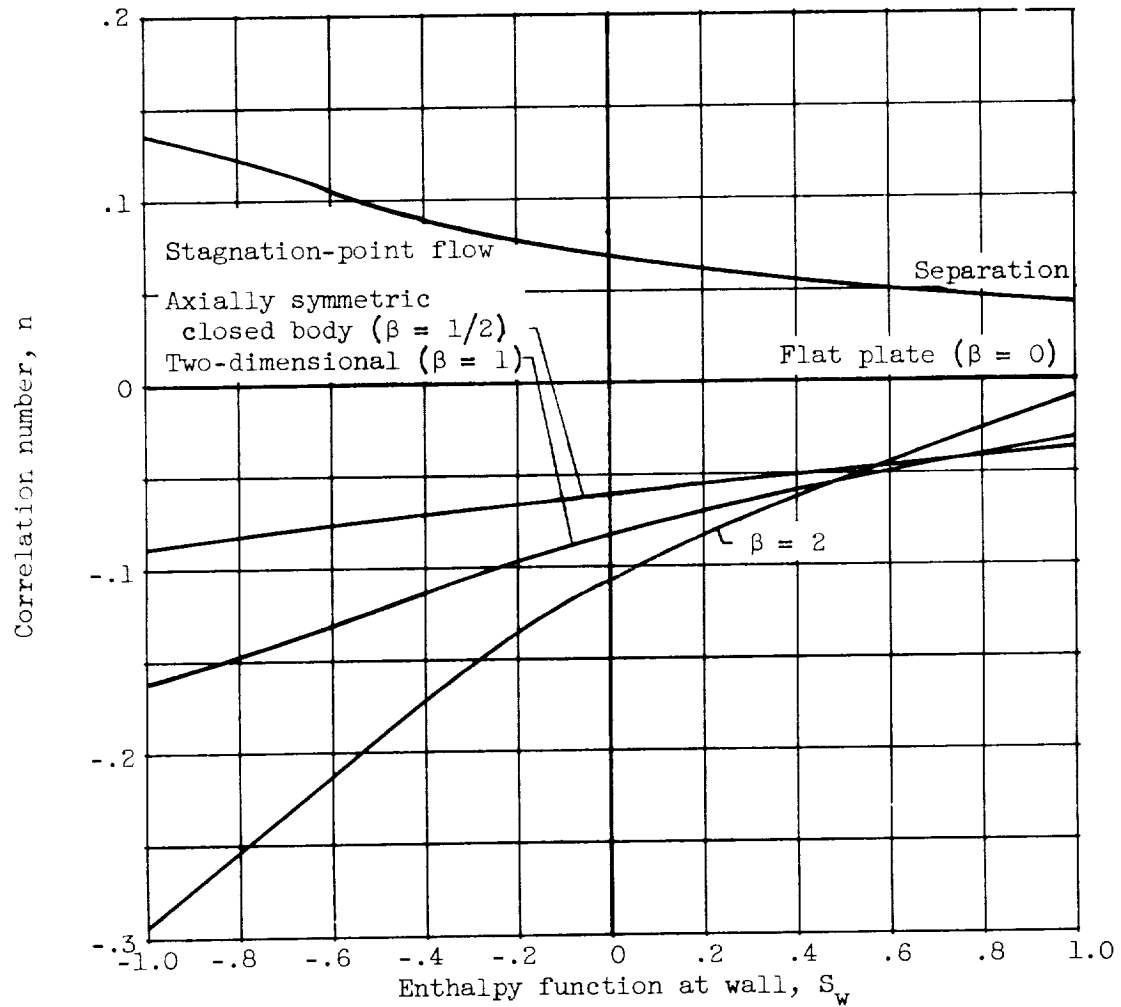


Figure 5. - Effect of wall temperature on correlation number for various pressure gradients.

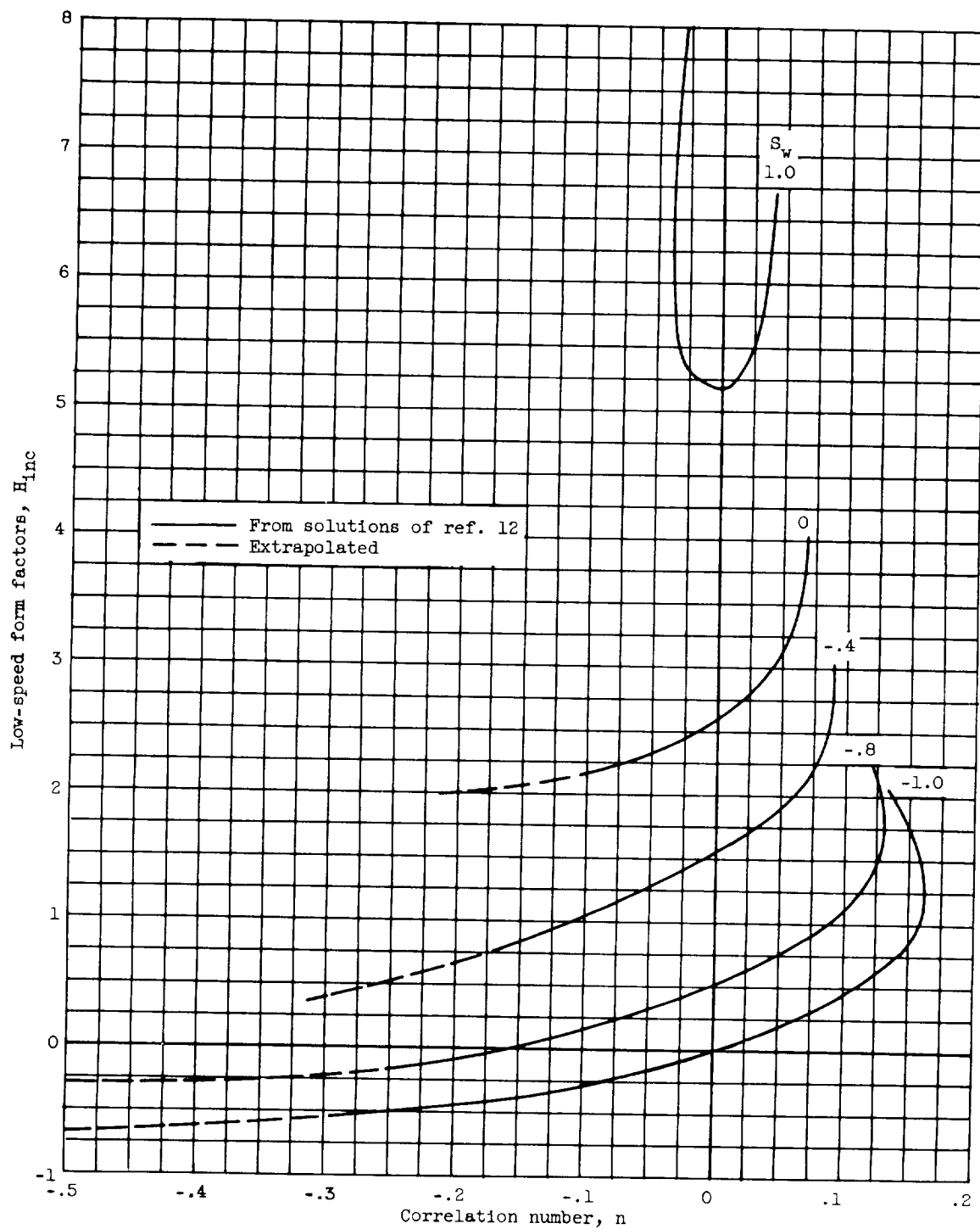


Figure 6. - Form-factor correlation.

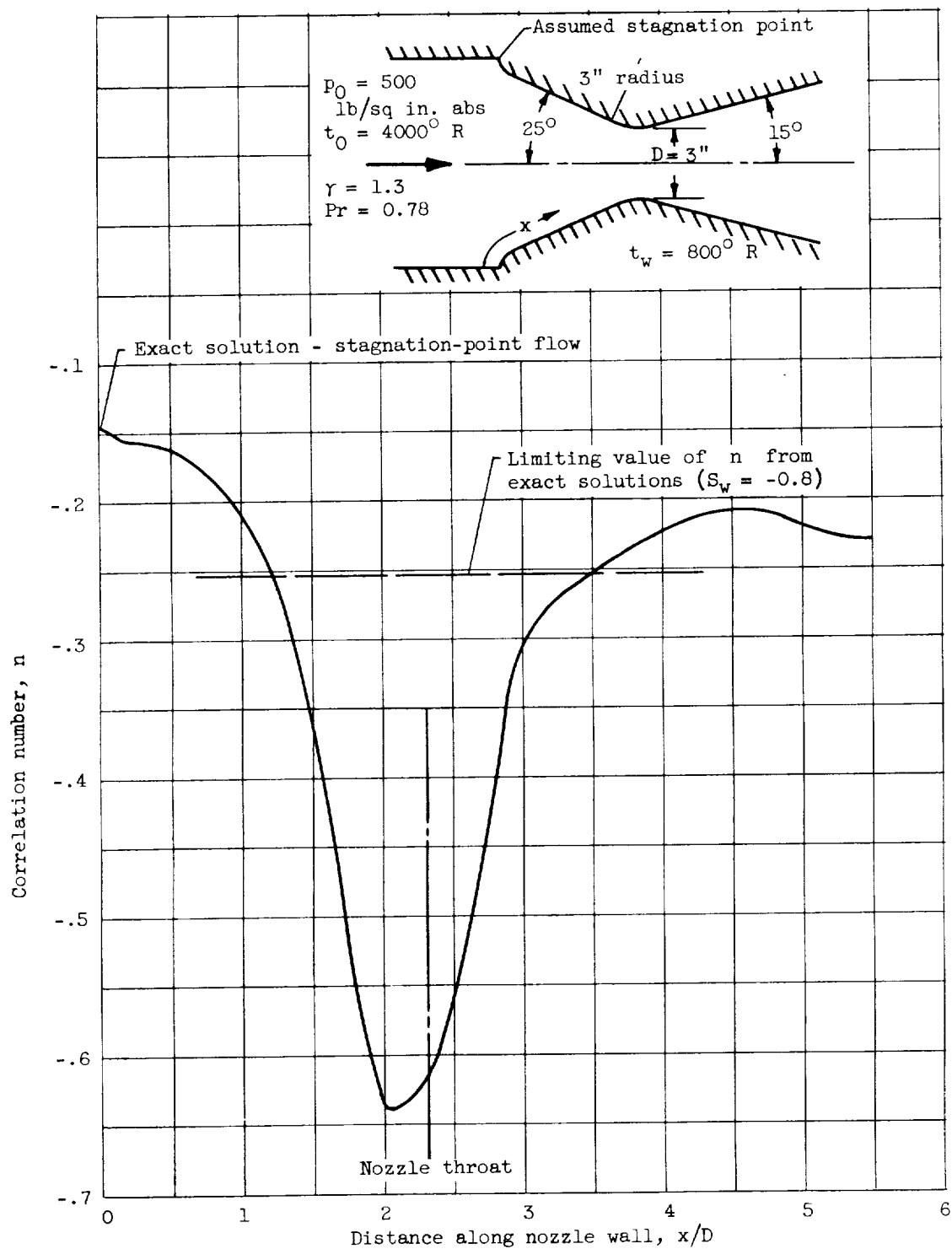


Figure 7. - Variation of correlation number in rocket nozzle.

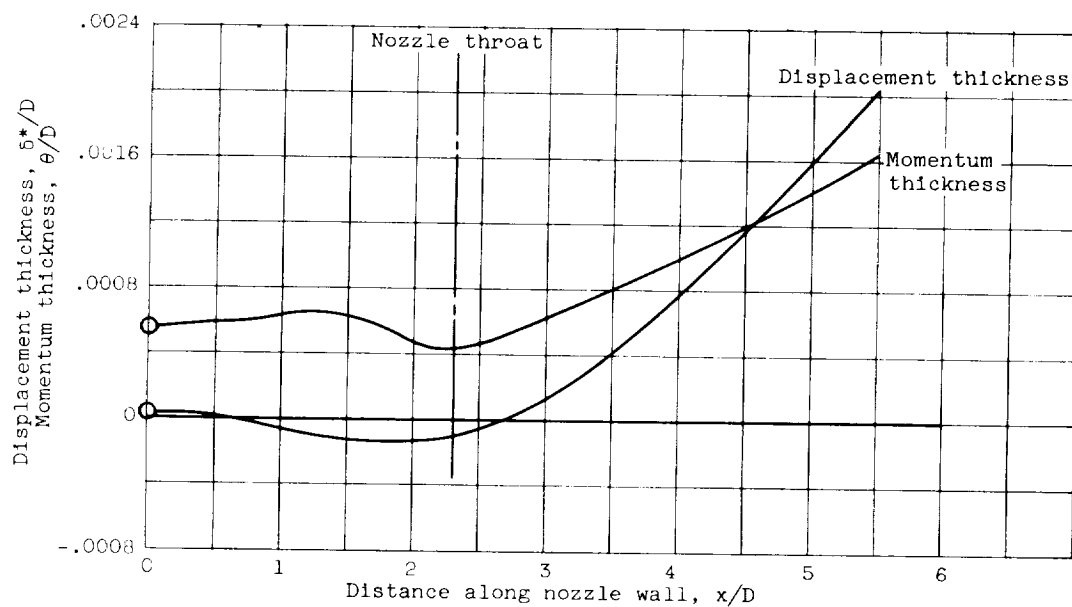
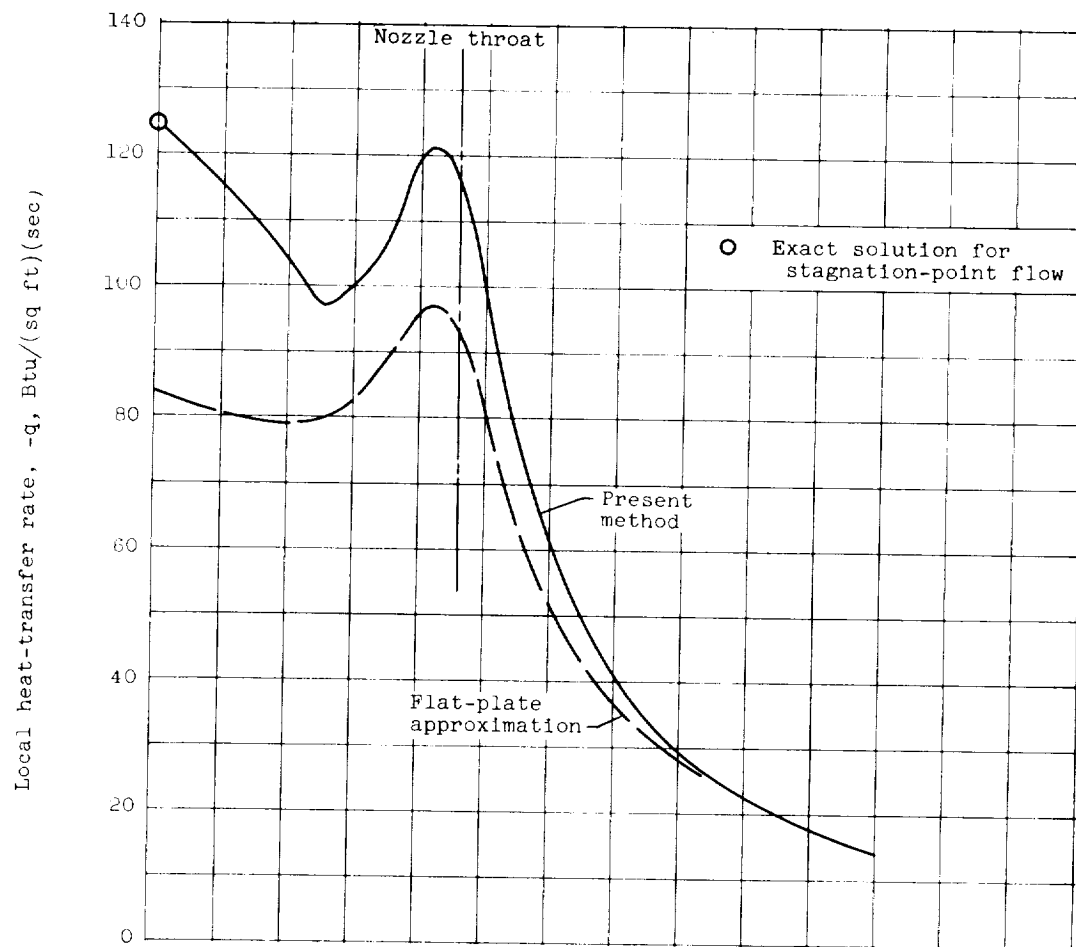


Figure 8. - Results of rocket-nozzle calculations.

